Angular and energy distribution of electrons from 15- to 150-keV H^0+He collisions

M. E. Rudd, J. S. Risley,* J. Fryar,† and R. G. Rolfes‡
Behlen Laboratory of Physics, University of Nebraska, Lincoln, Nebraska 68588
(Received 20 August 1979)

An electrostatic analyzer positioned at various angles has been used to measure absolute values of cross sections for electron production in collisions of neutral hydrogen atoms with helium as a function of the angle and energy of the ejected electrons. These cross sections are compared with corresponding ones for proton and electron impact to infer the mechanisms of electron production. A prominent peak in the energy distribution due to electron loss from the projectile occurs at an electron velocity equal to that of the projectile. At very low electron energies the similarity of the energy distribution to that due to electron impact suggests that the large cross section there is due to ionization of the target by the electron carried by the projectile. As with proton impact, the cross sections at low projectile velocities fall off approximately exponentially with the energy of the ejected electron, in agreement with the predictions of the electron promotion model.

I. INTRODUCTION

Numerous measurements have been made of cross sections for ejection of electrons from gases by protons as a function of the energy and angle of the emitted electrons,[1] and several reviews of this work are available.[2] These investigations have related the basic features of the distributions to various mechanisms by which electrons are ejected.

Besides the mechanisms of autoionization and the Auger effect, which yield discrete structures in the energy spectra of electrons, several mechanisms have been identified which produce the continuous spectrum. There is a binary collision peak which comes at an electron energy given by $E=4T\cos^2\theta - I$, where T is the energy an electron would have at the same velocity as the projectile and θ is the angle of ejection of the electron. This results from a collision in which the primary interaction is between the projectile and a loosely bound orbital electron in the target, the residual target ion serving only to provide a binding energy I. There is also a soft collision region at low electron energies resulting from large impact-parameter collisions which provide an impulse to the bound electrons just large enough to eject them. At high impact energies these two regions are well separated and can be described successfully by the binary-encounter approximation[1-3] or the Born approximation.[1-4] At lower energies the distinction between these regions disappears and the shape of the energy distribution is better described by an electron promotion model which yields an exponential dependence on electron energy.[5] An additional mechanism known as charge transfer to continuum states[6] operates in an intermediate range of energies. The electron is emitted in the frame of reference of the projectile rather than that of the target and thus has a velocity nearly equal to that of the projectile, thus yielding a peak in the forward direction at $E=T\cos^2\theta$. This peak is very large near $\theta=0$ but drops off quickly with angle and is difficult to detect at all beyond 30°.

Studies of this type have also been made for collisions in which the projectile carries one or more electrons, but only in cases where the projectile is charged. An electron may become detached from the projectile, make an elastic collision with the target, and appear at any angle with an energy $E=T$. This electron-loss mechanism was first noted by Wilson and Toburen[7] and investigated by Burch *et al.*,[8] by Stolterfoht *et al.*,[9] and by Drepper and Briggs.[10] Recently Toburen and Wilson[11] studied 0.3- to 2-MeV collisions of He^+ and He^{2+} with argon. They found that, in contrast to H^+ and He^{2+} collisions, the He^+ collisions produced a large electron-loss peak where the ejected electron velocity equalled that of the incident ion.

In the case of neutral particle impact, much less data is available. Total cross sections for ionization and electron loss have been measured for neutral hydrogen bomdarding helium by Solov'ev *et al.*,[12] Puckett *et al.*,[13] and McNeal *et al.*,[14] but no measurements have been made of the angular or energy distributions of ejected electrons from neutral-neutral collisions. The detail provided by this type of measurement is of great use in making progress toward an understanding of the mechanisms of electron production in such collisions. In addition to the theoretical interest, these data are of use in studies of aurora and other upper-atmospheric work, in energy-deposition and radiation-damage studies, and in other applied areas.

We present here measurements of cross sections

differential in angle and energy of the electrons from collisions of neutral hydrogen atoms with helium gas. Measurements of the target-gas density, beam intensity, detector efficiency, and geometry have been made to enable us to calculate absolute values of the cross sections. The projectile energies ranged from 15 to 150 keV, electron energies from 1.5 to 300 eV, and angles from 10° to 160°. No attempt was made to study the electrons from autoionization, which would require higher energy resolution and much smaller energy steps than we are using.

At the present time there are no theoretical calculations available which give doubly differential cross sections for neutral impact. Bates and Griffing[15] have calculated energy distributions of electrons using the Born approximation with hydrogen wave functions but only give the results for one impact energy. Bell, Dose, and Kingston[16] have calculated electron-loss cross sections for neutral hydrogen atoms on helium and vice versa using more realistic wave functions but only calculate total cross sections. Levy[17] has used experimental values of oscillator strengths in his Born-approximation calculations of electron-loss cross sections for hydrogen atoms on helium. It is hoped that the present data will stimulate additional work on neutral-impact calculations. In this paper we will attempt to explain the various features of the data by qualitative descriptions based on proton- and electron-impact work previously done.

II. EXPERIMENTAL METHOD

A diagram of the experimental apparatus is shown in Fig. 1. A beam of protons from a radio-frequency ion source is focused by a quadrupole lens, magnetically analyzed, and focused further by a second lens before entering the charge transfer cell shown. The cell provided a 50-cm path for the beam in hydrogen, which was chosen to be the neutralizing gas. Pressures of 2–40 mTorr were used, depending on the beam energy. High-speed differential pumping kept the pressure outside the gas cell below 4×10^{-5} Torr when the highest gas-cell pressure was used.

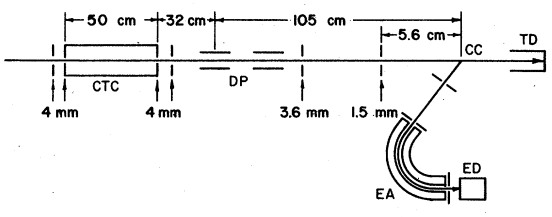

FIG. 1. Diagram of experimental arrangement: CTC, charge transfer cell; DP, deflection plates; CC, collision center; TD, thermal detector; EA, electrostatic analyzer; ED, electron detector.

Following the charge transfer cell the charged particles remaining in the beam were removed by electrostatic deflection. Two pairs of deflection plates, each pair 10.15-cm long and with a 1.8-cm plate spacing were available in the apparatus and both were used. Deflection voltages used ranged from 250 V at 15-keV beam energy to 750 V at 150 keV. These were typically five times the minimum potential necessary to deflect most of the charged component out of the beam. The same fields also served to quench metastable atoms and ionize highly excited atoms in the beam as discussed later.

The neutral beam then entered a collision chamber which was described earlier.[18] Three modifications have been made. The beam tube has been redesigned so as to put the last beam-defining aperture closer to the scattering center to give better beam definition and shorten the beam path in the target gas. The Faraday cup has been replaced by a neutral beam detector, and a Venetian-blind-type electron multiplier was used in place of the former electron detector. The neutral beam was measured by a secondary emission detector for most measurements. However, it was found that the secondary emission coefficient changed slowly with time and sometimes more abruptly when the vacuum was let down to change angles. Therefore, it was replaced by a thermal detector similar to one described by Gardon[19] and used by Stier, Barnett, and Evans.[20] A constantan foil disk of 0.021-mm thickness was fastened to the end of a $\frac{1}{4}$-in copper cylinder. A fine copper wire was spot welded to the center of the Constantan disk on the side opposite from where the beam was incident. This formed one junction of a thermocouple, the other junction being the periphery of the Constantan disk where it was joined to the copper tube. Using the thermal detector as a Faraday cup with a proton beam for calibration, we found the sensitivity to be 0.0167 V/W and the time constant about 1 sec. Signals, typically a few microvolts to about 100 μV, were amplified by a specially designed chopper-stabilized amplifier, read on an electrometer, and integrated. At the lowest beam powers some fluctuations, due to thermal emf's in the feed-through at the chamber wall, were noticed but these were minimized by shielding the feed-throughs from air currents. With this system, beam currents as small as 10^{-8} A could be read at the lowest beam energy used, 15 keV.

Using the thermal detector, runs were made at each angle and at one or more beam energies in order to normalize the data previously taken with

the secondary emission detector. In most cases the corrections were within 15%, but in a few cases larger adjustments had to be made.

Electrons from the scattering center entered the 127° electron energy analyzer after being collimated to within ±1.4° by two slits. In order for the geometry to be well defined, this region was maintained free of electric fields by gold plating all the inside surfaces of the inner chamber and the path leading to the analyzer. Magnetic fields were reduced to under 5 mG in the region by carefully adjusting the currents in three mutually perpendicular Helmholtz coils surrounding the chamber and analyzer while reading out the fields with a sensitive rotating-coil Gaussmeter. No preacceleration was used and the electrons were analyzed at the same energy at which they were produced. The slits in the analyzer were made of gold, and the analyzer electrodes were gold plated to minimize contact potentials and to prevent oxide coatings from forming. The analyzer had a full width at half maximum energy resolution of 5.7%.

After leaving the analyzer, electrons were accelerated by about 100 V to the first dynode of an EMI 9642/3B electron multiplier. Pulses of electrons were amplified by a fast charge-sensitive preamplifier mounted at the back of the electron multiplier. Pulses were then further amplified and counted on a multiscalar. The analyzer power supply was programmed by a hand calculator which also controlled the address of the multiscalar.[21]

The efficiency of the electron detector (which was 70–80%) was measured from time to time by comparing the current from a filament through an aperture to the count rate of electrons through a much smaller hole of measured size. The target gas, supplied from cylinders at 99.995% purity, was reduced in pressure by an all-metal regulator, passed through a metal gas line and needle valve to the chamber. The pressures were measured by an MKS Baratron capacitance manometer. Corrections were made for thermal transpiration due to the fact that the manometer head was heated and for the nonzero reference pressure for the manometer. For each run, a second run was made without the target gas and the corresponding counts subtracted.

In our earlier proton impact work we made a correction for the fraction of the beam that was neutralized during its passage through the target gas and thus was not read by the electrometer connected to the Faraday cup. In the present case, charge transfer collisions populated the neutral beam with a small fraction (less than 3%) of protons but since the thermal detector responded to them in the same way as to neutrals, no correction was needed. If the charge transfer took place before the collision center a correction would be needed if the cross sections for electron ejection by protons and neutrals were different. However, because the fraction of the beam which is charged is very small, no correction was made. Electron absorption between the scattering center and electron detector required a correction ranging from 0 to as much as 9% in some cases.

The uncertainty in the pressure measurement was about 10% and a similar uncertainty was present in the measurement of the detector efficiency. While the uncertainty in the calibration of the thermal detector for the beam was only about 2%, some variation in the calibration constant was noted with changing position and focus of the beam. In addition, stray thermal emf's limited the accuracy at the lower beam energies. We will assign a 10% uncertainty to the beam measurements above 30 keV with an increase to 20% at 15 keV.

As in previous measurements of this type, the count rates decreased as the electron energy was increased until statistical uncertainties became large. At low electron energies, small residual fields in the chamber and analyzer caused large discrepancies in the data taken at different times. Because of difficulties in controlling this problem the uncertainty below 10 eV increases to about a factor of 2 at 2 eV.

Errors in the measurement of geometrical factors such as solid angle, length of beam viewed, and energy resolution were of the order of 1%. The overall uncertainty, then, is 17% above 30 keV increasing to 25% at 15 keV, with additional uncertainties at the lower electron energies as noted above. Since the cross sections are usually largest at the lowest electron energies, the cross sections integrated over electron energy will have an additional uncertainty, amounting perhaps to as much as 40%.

III. EXCITED ATOMS

The question arises as to whether the neutral beam which caused the ejection of electrons at the collision center contained an appreciable number of atoms which were not in the ground state. Since the distance the beam must travel from the charge transfer cell to the collision center is about 1.4 m, the drift time varied from $\frac{1}{3}$ to 1×10^{-6} sec. Hydrogen atoms in the lower excited states have mean lifetimes of the order of 10^{-8} sec and so will have almost completely decayed to the ground state before reaching the collision center. There are, however, two cases which must be investigated; metastable $2s$ atoms and atoms in high-n states (the so-called "Rydberg atoms").

A. Metastable atoms

From the cross sections for charge transfer to the $2s$ state and to all other states we can calculate the fraction of the beam in the $2s$ state as it emerges from the charge transfer cell. The thickness of the gas used in the cell is such that the beam is almost completely equilibrated as regards the $2s$ state and the calculated fraction varies from about 2% at 15 keV to 16% at 150 keV. The electrostatic field used to deflect ions from the beam also serves, in our apparatus, as a quenching field by providing Stark mixing with the $2p$ state followed by a rapid decay to the ground state. Sellin[22] has given an equation for the lifetime of a $2s$ atom in an electric field in terms of the field strength, the Lamb shift, and the $2p$ lifetime. For our experiment the $2s$ lifetimes varied from 1.6×10^{-8} sec at the field used at 15 keV to 0.6×10^{-8} sec at 150 keV. Considering the time the beam spends between the deflection plates, we calculate an attenuation varying from 5×10^{-4} to 3×10^{-3}. Combining with the original metastable fractions we get a $2s$ population entering the scattering chamber varying from 8×10^{-6}% at 15 keV to 4×10^{-4}% at 150 keV. These fractions are too small to affect the measured cross sections.

B. Rydberg atoms

Bethe and Salpeter[23] show that the lifetime of a hydrogen atom for a fixed l value is proportional to n^3. Also from their data we can estimate that if $l=n-1$, the lifetime varies approximately as n^5. Thus by the time n reaches 7 the lifetime of high-angular-momentum states is great enough that the natural decay of excited atoms no longer greatly reduces the population of Rydberg atoms before reaching the scattering center. The field which quenches the $2s$ states is not of much help in this case since the states which might mix with the long-lived states also have long lifetimes themselves.

Rydberg atoms can be ionized by static fields of sufficient magnitude. The threshold for field ionization is given by Kleppner[24] as $E_0=3.2\times10^8/n^4$ in V/cm. The efficiency of ionization by this method goes essentially from zero at small fields to 100% at this point. For the fields we use for deflection of the charged component of the beam, all Rydberg atoms with n above about 30 or 40 would be eliminated by this process. We need be concerned, then, only with Rydberg atoms with n in the range of about 7–40.

From data of Riviere and Sweetman[25] we find that for protons passing through hydrogen gas the largest fraction of Rydberg atoms occurs at about 50 keV and for $n=7$ is 0.1% decreasing to 5×10^{-6} at $n=40$. Even if we sum over all states from 7 to 40 we have only about 0.4% of the neutral beam populated by Rydberg atoms, a number too small to affect our measurements.

IV. EXPERIMENTAL CHECKS

To check on the control of metastable and Rydberg atoms as well as on other possible effects, a number of experimental parameters were varied to see if they affected the measured values of the cross sections.

Using a 50-keV beam, the deflection plate potential was varied from 200 to 700 V. The apparent cross sections at various electron energies were found to vary by 6–16% but not in any systematic way. Since this variation was within the experimental uncertainty, it was not considered further. At the same beam energy the pressure in the charge transfer cell was varied from 2 to 23 mTorr, but this caused variations in cross sections ranging only up to 8%.

A rather extensive set of tests was made to see the effect of varying the target-gas pressure. Runs over the electron energy range at pressures of 0.5 to 3.0 mTorr were made at different beam energies and angles. A general decrease in apparent cross section was noted as the pressure increased. The size of the decrease did not depend on the electron energy or the angle but did seem to depend on the beam energy, going from about 22% at 30 keV to 13% at 100 keV. It is not likely that this pressure effect is due to incorrect accounting for electron absorption since the cross section for electron absorption is strongly dependent on electron energy, while the effect measured was not. The thickness of target gas before the collision center is less than 6 cm, so no appreciable buildup of excited state atoms is to be expected, and since their initial fractions have been shown to be small any reduction by the target gas should have a negligible effect. While we have no explanation for this dependence on pressure, the variability it causes in our data should be small since the runs from which the final data were derived were all taken at pressures between 0.4 and 0.7 mTorr.

Because there is a small magnetic field gradient over the region occupied by the collision chamber and analyzer we made runs with the field nulled at various points on the electron trajectory from the collision center to the detector. The maximum spread in the data was ±10% at 10 eV and was negligible at higher energies.

V. EXPERIMENTAL RESULTS

Measurements were made at all combinations of 7 beam energies from 15 to 150 keV, 8 angles

TABLE I. Singly differential cross sections (integrated over angles) for electron production in H^0+He collisions, in m^2/eV.

Electron energy (eV)	Projectile Energy (keV) 15	20	30	50	70	100	150
1.5	1.19-21[a]	8.15-22	8.00-22	6.97-22	7.27-22	6.24-22	5.07-22
2.0	1.06-21	7.83-22	6.69-22	5.88-22	5.64-22	5.40-22	4.16-22
3.0	1.16-21	8.29-22	6.35-22	5.55-22	4.09-22	3.68-22	3.47-22
5.0	1.06-21	8.63-22	6.87-22	4.76-22	3.56-22	2.72-22	2.11-22
7.5	8.08-22	8.05-22	7.48-22	4.97-22	3.34-22	2.36-22	1.44-22
10.0	5.52-22	6.58-22	6.89-22	4.84-22	3.17-22	2.10-22	1.25-22
15.0	2.45-22	3.44-22	5.53-22	4.75-22	3.23-22	1.97-22	1.01-22
20.0	1.27-22	1.91-22	3.19-22	4.41-22	3.44-22	1.98-22	9.34-23
30.0	4.63-23	7.46-23	1.31-22	2.83-22	3.15-22	2.09-22	9.23-23
50.0	7.46-24	1.42-23	2.93-23	7.63-23	1.31-22	1.90-22	9.65-23
75.0	1.13-24	2.57-24	6.02-24	2.14-23	3.97-23	7.10-23	1.01-22
100.0	1.90-25	4.78-25	1.69-24	6.48-24	1.47-23	2.77-23	4.65-23
130.0		7.62-26	4.31-25	1.62-24	5.27-24	1.10-23	1.72-23
160.0				5.30-25	1.84-24	4.70-24	7.23-24
200.0					4.51-25	1.58-24	2.78-24
250.0					7.77-26	4.45-25	1.17-24
300.0					1.93-26	1.26-25	4.21-25
Total (m^2)	1.36-20	1.37-20	1.59-20	1.80-20	1.78-20	1.68-20	1.19-20

[a] The designation 1.19-21 means 1.19×10^{-21}.

from 10° to 160°, and 17 electron energies from 1.5 to 300 eV. Dependences of the doubly differential cross sections for electron ejection on these three parameters are presented in this section along with cross sections integrated over all angles, all electron energies, or both. Tables of the doubly differential cross sections may be obtained from M.E.R. on request. Cross sections integrated over angle are given in Table I along with total electron production cross sections.

The energy distribution of electrons from 150-keV impacts is shown for various angles in Fig. 2 along with the distribution integrated over all angles. At the small angles a rapid drop is followed by a rise to a maximum at the point where the ejected electron velocity is approximately equal to the projectile velocity. At larger angles the maximum becomes less pronounced and in the backward angles it is only a shoulder on the monotonically decreasing curve. The curves for 110° and 130° have been omitted for clarity as they fall close to the 160° curve.

In Fig. 3, the 10° 150-keV distribution is compared to the corresponding proton impact data of Rudd and Jorgensen.[18] Since high-energy electrons come primarily from close collisions, we would expect protons and neutral hydrogen atoms to produce similar effects at a sufficiently large velocity. Indeed, we see that the cross sections

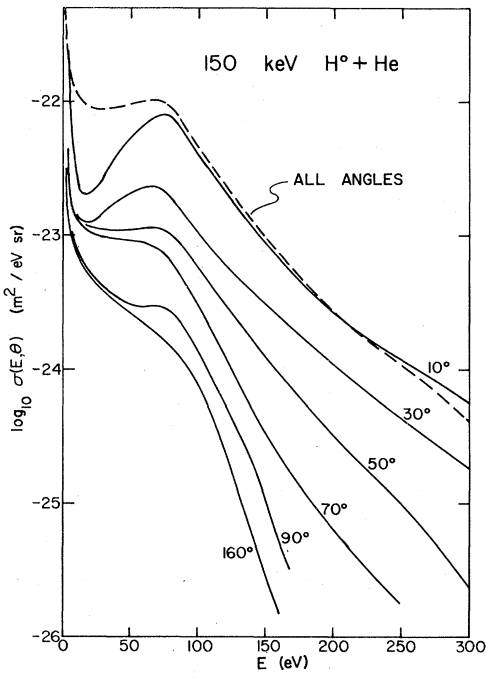

FIG. 2. Energy distribution of electrons at various angles for 150-keV neutral-hydrogen impacts on helium. Dotted line show the singly differential cross sections, integrated over all angles, in m^2/eV on the same numerical scale.

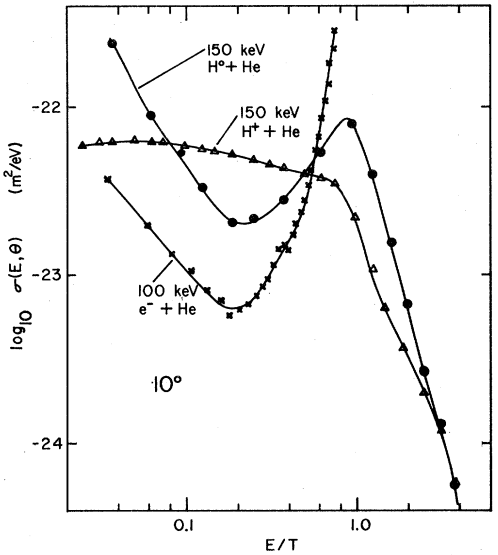

FIG. 3. Comparison of energy spectrum of electrons from 150-keV neutral-hydrogen and proton impact and 100-eV electron impact on helium. Electrons ejected at 10° relative to the beam. T is the energy of an electron with the same velocity as the incident particle. Proton data are from Ref. 18 and electron data are from Ref. 26.

at large ejection energies are nearly the same. This is also the case at other angles. At an intermediate electron energy where the velocities of the ejected electron and projectile are equal we find a peak in the neutral-impact data which is due to electrons stripped from the projectile and elastically scattered from the target atoms. As seen in Fig. 2, this electron-loss peak is most prominent in the forward direction where the elastic scattering cross section is largest.

Low-energy electrons come from large-impact-parameter collisions. For these the screening effect of the electron on the projectile should make the cross sections small, and one notes that in the 7–20 eV region the cross sections for neutral impact are smaller than for ion impact. At the very lowest electron energies, however, there is again a rise in the neutral-impact cross sections. This may be attributed to target ionization caused by the electron carried by the projectile. Supporting this idea is the fact that for equal impact velocities, the energy dependence of the electron and neutral-impact ionization cross sections are similar in shape as shown in Fig. 3. Here we have plotted the 10° data of Rudd and DuBois[26] for 100-eV electron impact since those data were the closest in velocity to the 150-keV neutral data which were available. When data integrated over all angles are compared, the shapes of the neutral- and electron impact distributions are even more alike and, in addition, the magnitudes are closer.

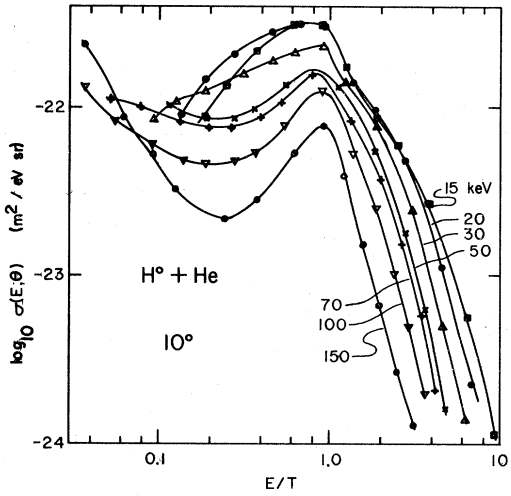

FIG. 4. Comparison of energy distribution of electrons ejected at 10° by various energies of neutral hydrogen atoms.

If the cross sections scale as $1/T$ (as in the Rutherford equation), then, taking account of the somewhat different velocities, the ratio of neutral to electron cross sections is in the range of 1.1 to 1.8 over nearly the entire energy range.

In Fig. 4 we compare 10° neutral data for various impact energies and note that the maxima in the curves are slightly lower in energy than they would be if the ejection velocity were exactly equal to the projectile velocity. Also the maximum becomes broader and shifts to lower energies as

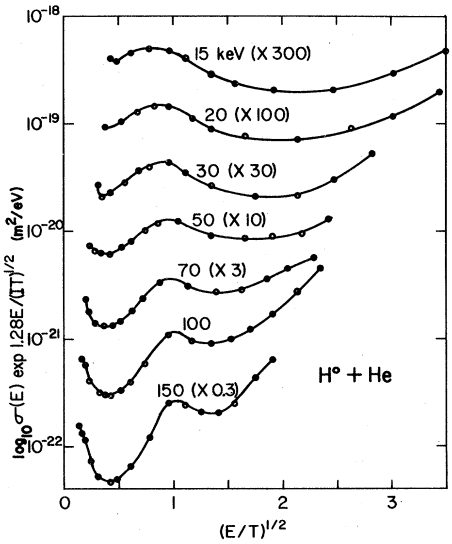

FIG. 5. Singly differential cross sections, integrated over all angles for ejection of electrons from helium by neutral hydrogen atoms of various energies. Cross sections have been multiplied by an exponential function (see text) to eliminate the rapid decrease with energy.

the impact energy is reduced. This is probably due to the influence of the binding energy. Cross sections above the peak scale quite accurately and when plotted versus $E/T^{1/2}$, fall close to a universal curve.

In Fig. 5 we show energy distributions of singly differential cross sections resulting from an integration over angles. In an earlier publication[5] it was shown that the rapid decrease with energy which often obscures details of structure in the energy distributions can be compensated for by multiplying the cross sections by $\exp \alpha E/(IT)^{1/2}$, where I is the ionization potential of the target, α is a dimensionless length parameter equal to 1.28 for helium, and T is $\frac{1}{2}m_e v_p^2$, where m_e is the mass of the electron and v_p the velocity of the projectile. This multiplier has been applied to the data in Fig. 5 to level out the curves. This procedure reduces the variation over the energy range from over four orders of magnitude to a range of 2–2.5 at the lower impact energies, indicating that the exponential model developed for proton impact also seems to apply to neutral impact.

To compare the neutral data to the proton impact results presented earlier,[4,18] Fig. 6 shows the ratio of the cross sections for the two cases integrated over angles. At the higher energies the electron-loss peak at $E = T$ is very obvious but broadens out and disappears as the energy is lowered. At 15 keV the ratio is nearly constant at 2.5–3.0 except at the very lowest electron energies where the data are uncertain. At low

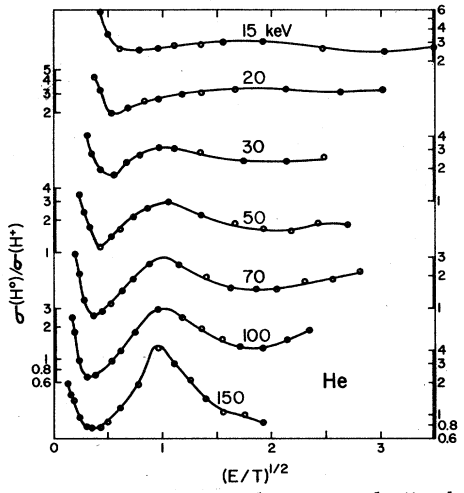

FIG. 6. Cross sections for electron production by hydrogen atoms of various energies integrated over all angles as a function of the ejected electron energy. We have divided cross sections by the corresponding cross sections due to proton impact using data of Rudd and Madison (Ref. 4) and Rudd and Jorgensen (Ref. 18).

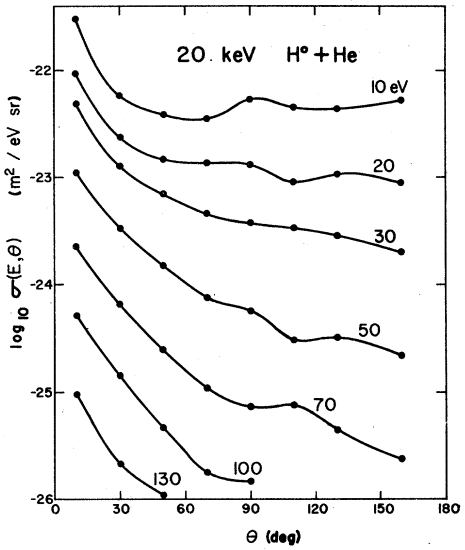

FIG. 7. Angular distribution of electrons of various energies from 20-keV neutral impacts.

impact velocities ionization probably proceeds via a promotion mechanism[5] and the availability of more electrons in the neutral-impact case would be expected to cause a larger cross section.

Typical angular distributions for various electron energies for 20-keV H^0 impact are shown in Fig. 7. We cannot say whether the structure which appears in some of the curves is real or only a result of the fact that when the angle was changed the vacuum had to be let down, thus possibly affecting the detector efficiency. There is some

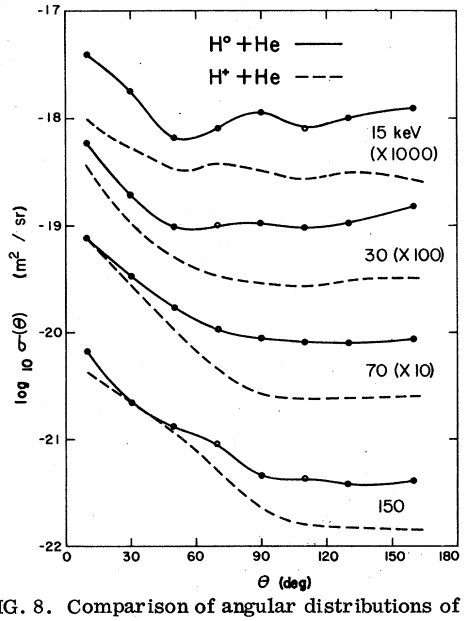

FIG. 8. Comparison of angular distributions of electrons of all energies ejected from helium by neutral hydrogen atoms and protons of various energies.

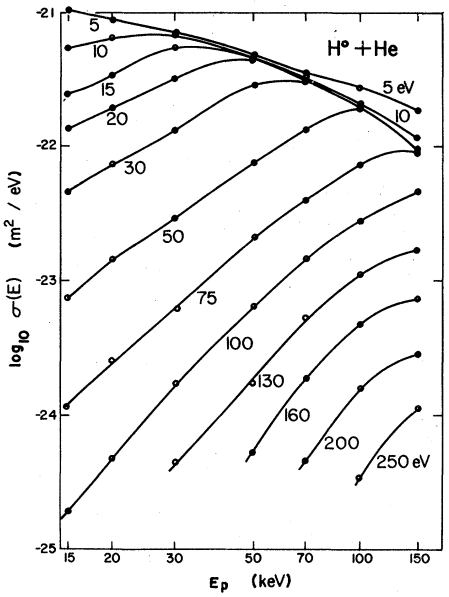

FIG. 9. Cross sections, integrated over all angles, for ejection of electrons of various energies as a function of projectile energy E_p.

other evidence for structure in the angular distributions of electrons from low-energy projectiles,[5] but until measurements can be made with a finer angular grid nothing definite can be said. In Fig. 8 angular distributions integrated over all electron energies for neutral impact are compared with those for proton impact. The distributions from neutrals are more isotropic except at the lowest energy.

What corresponds in ionization to excitation functions are plotted in Fig. 9. This shows the variation with impact energy of the cross section for ejection of electrons of various energies. As expected, the maximum in the curves shifts to higher impact energies for higher electron energies. More surprising was the existence of a nearly common value at the top of the graph for a range of electron energies.

Our cross sections when integrated over both angle and energy yield total cross sections for electron production which may be compared to the results of more direct methods of measurement. Figure 10 shows the present results along with experimental data from Solov'ev *et al.*,[12] Puckett *et al.*,[13] and McNeal *et al.*[14] Our data agree well with the other measurements at high energies and reasonably well with the data of McNeal *et al.* at the low energies. Also shown on the same graph are the results of calculations using the Born approximation. Bell *et al.*[16] have calculated electron-loss cross sections for hydrogen atoms incident on helium and for helium atoms incident on atomic hydrogen. By proper scaling and addition of the two cross sections one can obtain the total cross sections for electron production by fast hydrogen atoms incident on helium and these are shown as the dashed line. The theory generally underestimates the cross sections. A different calculation of the electron-loss cross sections of H^0 on He has been made by Levy.[17] Combining his results with the cross sections for ionization of helium from Bell *et al.*, we get a result which agrees generally within 30% of our data, although it is still much lower than McNeal's results at low energies.

VI. CONCLUSIONS

Some of the mechanisms for electron production in proton impact are seen to be operating in the neutral-impact case but additional ones are also apparent from the data. The energies studied in this experiment were too low to see more than just the beginning of the binary collision peak and the results are better described by the exponential

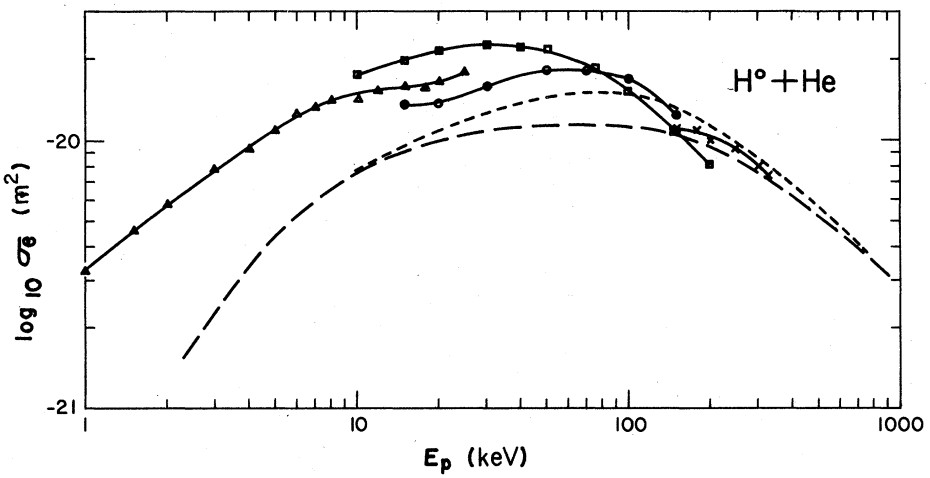

FIG. 10. Total cross section for electron production σ_e by neutral hydrogen atom impact on helium vs projectile energy: Circles, present data; squares, data of Solov'ev *et al.* (Ref. 12); triangles, data of McNeal *et al.* (Ref. 14); crosses, data of Puckett *et al* (Ref. 13); dashed line, calculations of Bell *et al.* (Ref. 16); dotted line, calculations of Levy (Ref. 17).

energy distribution resulting from a promotion mechanism. Charge transfer to continuum states could not be seen since the peak due to that mechanism is overshadowed by the larger peak due to elastically scattered electrons detached from the neutral projectile. This peak was quite prominent at the higher energies in this study but became less so at lower energies. We have explained a rise in the cross sections at very low energies in terms of ionization of the target caused by the electron carried by the projectile and justified this by comparison of the shape of the energy distribution with that of equal-velocity electrons.

ACKNOWLEDGMENTS

This work was done with the support of National Science Foundation Grant No. PHY-77-27, 523. The authors wish to thank E. P. Rudd for constructing several of the electronic circuits used and for writing the data processing program. We also appreciate the helpful suggestions made by B. Van Zyl. K. Bauer and B. Krauter assisted in taking data.

*Present address: Dept. of Physics, North Carolina State Univ., Raleigh, N. C. 27607.

†Present address: Dept. of Physics, New Univ. of Ulster, Coleraine Co., Londonderry, North Ireland BT 52 1SA.

‡Present address: Dept. of Physics, Univ. of Kentucky, Lexington, Ky. 40506.

[1]See, e.g. M. E. Rudd, L. H. Toburen, and N. Stolterfoht, At. Data Nucl. Data Tables 18, 413 (1976); T. L. Criswell, L. H. Toburen, and M. E. Rudd, Phys. Rev. A 16, 508 (1977); L. H. Toburen, Steven T. Manson, and Yong-Ki Kim, *ibid.* 17, 148 (1978) and references contained therein.

[2]Gennadi N. Ogurtsov, Rev. Mod. Phys. 44, 1 (1972); M. E. Rudd and J. H. Macek, Case Stud. At. Phys. 3, 47 (1972), M. E. Rudd, Radiat. Res. 64, 153 (1975); N. Stolterfoht, in *Topics in Current Physics*, Vol. 5, edited by I. A. Sellin (Springer-Verlag, Berlin, 1978), p. 155.

[3]M. E. Rudd, D. Gregoire, and J. B. Crooks, Phys. Rev. A 3, 1635 (1971).

[4]M. E. Rudd and D. H. Madison, Phys. Rev. A 14, 128 (1976).

[5]M. E. Rudd, Phys. Rev. A 20, 787 (1979).

[6]J. Macek, Phys. Rev. A 1, 235 (1970).

[7]W. E. Wilson and L. H. Toburen, Phys. Rev. A 7, 1535 (1973).

[8]D. Burch, H. Wieman, and W. B. Ingalls, Phys. Rev. Lett. 30, 823 (1973).

[9]N. Stolterfoht, D. Schneider, D. Burch, H. Wieman, and J. S. Risley, Phys. Rev. Lett. 33, 59 (1974).

[10]F. Drepper and J. S. Briggs, J. Phys. B 9, 2063 (1976).

[11]L. H. Toburen and W. E. Wilson, Phys. Rev. A 19, 2214 (1979).

[12]E. S. Solov'ev, R. N. Il'in, V. A. Oparin, and N. V. Fedorenko, Sov. Phys. JETP 15, 459 (1962).

[13]L. J. Puckett, G. O. Taylor, and D. W. Martin, Phys. Rev. 178, 271 (1969).

[14]R. J. McNeal, D. C. Clark, and R. A. Klingberg, Phys. Rev. A 2, 131 (1970).

[15]D. R. Bates and G. Griffing, Proc. Phys. Soc. London A 66, 961 (1953); 68, 90 (1955).

[16]K. L. Bell, V. Dose, and A. E. Kingston, J. Phys. B 2, 831 (1969). See also H. S. W. Massey and H. B. Gilbody, *Electronic and Ionic Impact Phenomena* (Oxford University, London, 1974), Vol. IV, p. 2444.

[17]H. Levy II, Phys. Rev. 185, 7 (1969).

[18]M. Eugene Rudd and Theodore Jorgensen, Jr., Phys. Rev. 131, 666 (1963).

[19]Robert Gardon, Rev. Sci. Instrum. 24, 366 (1953).

[20]P. M. Stier, C. F. Barnett, and G. E. Evans, Phys. Rev. 96, 973 (1954).

[21]John S. Risley, J. Phys. E 10, 464 (1977).

[22]I. A. Sellin, Phys. Rev. 136, A1245 (1964).

[23]H. A. Bethe and E. F. Salpeter, *Quantum Mechanics of One- and Two-Electron States* (Springer-Verlag, Berlin, 1957), p. 266.

[24]D. Kleppner, *Atomic Physics* 5, edited by R. Marrus, M. Prior, and H. Shugart (Plenum, New York, 1976), p. 269.

[25]A. C. Riviere and D. R. Sweetman, in Proceedings of the Sixth International Conference on Ionization Phenomena in Gases, Paris, 1963, Vol. 1, p. 105 (unpublished).

[26]M. E. Rudd and R. D. DuBois, Phys. Rev. A 16, 26 (1977).